Lipid droplets modulate proteostasis, SQST-1/SQSTM1 dynamics, and lifespan in *C. elegans*

Anita V. Kumar[#,1], Joslyn Mills[#, 1], Wesley M. Parker[#, 1], Joshua A. Leitão[#, 1], Diego I. Rodriguez[, 1], Celeste Ng[, 1], Rishi Patel[, 1], Joseph L. Aguilera[, 1], Joseph R. Johnson[, 1], Shi Quan Wong[, 1] and Louis R. Lapierre[*, 1,2]

[#]: Equal contributions

[*]**:** Correspondence addressed to L.R.L. (louis.rene.lapierre@umoncton.ca)

1: Department of Molecular Biology, Cell Biology and Biochemistry, Brown University, 185 Meeting St., Providence, Rhode Island 02912, USA

2 : Centre de Médecine de Précision du Nouveau Brunswick, Département de chimie et biochimie, Université de Moncton, 27 rue Providence, Moncton, New Brunswick, E1C 8X3, Canada

ABSTRACT

The ability of organisms to live long depends largely on the maintenance of proteome stability via proteostatic mechanisms including translational regulation, protein chaperoning and degradation machineries. In several long-lived *Caenorhabditis elegans* strains, such as insulin/IGF-1 receptor *daf-2* mutants, enhanced proteostatic mechanisms are accompanied by elevated intestinal lipid stores, but the role of lipid droplets in longevity has remained obscure. Here, while determining the regulatory network of the selective autophagy receptor SQST-1/SQSTM1, we unexpectedly uncovered a novel role for lipid droplets in proteostasis and longevity. Using an unbiased genome-wide RNAi screening approach, we identified several SQST-1 modulators, including proteins found on lipid droplets and those prone to aggregate with age. SQST-1 accumulated on lipid droplets when autophagy was inhibited, suggesting that lipid droplets may serve a role in facilitating selective autophagy. Expansion of intestinal lipid droplets by silencing the conserved cytosolic triacylglycerol lipase gene *atgl-1/ATGL* enhanced autophagy, and extended lifespan in an HSF-1/HSF1-dependent and CDC-48/VCP-dependent manner. Silencing *atgl-1* mitigated the

age-related accumulation of SQST-1 and reduced overall ubiquitination of proteins. Reducing *atgl-1* also improved proteostasis in proteotoxicity models of neurodegenerative diseases. Subcellular analyses revealed that lipid droplets unexpectedly harbor more soluble ubiquitinated proteins than the cytosol. Accordingly, low lipid droplet levels exacerbated the proteostatic collapse when autophagy or proteasome function was compromised. Altogether, our study uncovers a key role for lipid droplets in *C. elegans* as a proteostatic mediator that reduces protein ubiquitination, facilitates autophagy, and promotes longevity.

INTRODUCTION

One of the major hallmarks of aging is the accumulation of damaged proteins that progressively compartmentalize in inclusions and aggregates[1]. In the nematode *C. elegans*, numerous proteins display impaired solubility with age[2,3]. This phenomenon suggests that mechanisms that mediate protein stabilization, such as chaperone-mediated folding and post translational modifications, actively contribute to somatic maintenance by preventing the collapse of the proteome[4,5]. The enhanced proteasomal[6] and autophagic[7,8] capacities, the increased chaperone function[9] and alterations in ribosomal biogenesis[10] and function[11,12] in long-lived nematodes support the notion that the balance between synthesis, folding, and efficient clearance of proteins is important for conferring organismal longevity.

Generally, proteins destined for degradation are tagged via poly-ubiquitination and recognized by ubiquitin binding domain-containing proteins that direct cargo toward proteasomal or autophagic degradation. The autophagy receptor, Sequestosome 1 (SQST-1/SQSTM1) is a well-established and conserved mediator of cargo recognition, which includes ubiquitinated targets[13]. The SQST-1-cargo complex can interact with the autophagosome proteins LGG-1/GABARAP and LGG-2/LC3 to enable cargo sequestration in the nascent autophagosome[14]. Notably, SQST-1/SQSTM1 has emerged as a potential lifespan modulator in nematodes and flies[15-17]. Additionally, selective autophagy of mitochondria has been linked to longevity[18], suggesting that

53 autophagic degradation of specific cargos and organelles is beneficial against organismal aging.
54 Although SQST-1/SQSTM1 has been implicated in the selective clearance of aggregated
55 proteins[19], much remains to be understood about the modulation of this autophagy receptor, its
56 cargoes, and the nature and extent of its contribution to lifespan.
57 In nematodes, intestinal cells have a unique role in autophagy-mediated longevity as they manage
58 nutrient influx and signals from neurons[20] and the germline[21] to coordinate appropriate responses
59 necessary for organismal survival. In particular, intestinal autophagy genes are required for
60 lifespan extension[22] by maintaining intestinal tissue integrity and proteostasis. Intestinal cells are
61 also sites of dynamic lysosomal function[23-26] that mediate specific longevity-associated lipid
62 signaling[27-29]. Intriguingly, several established long-lived animals including *daf-2*, *glp-1* and *rsks-*
63 *1* mutants also maintain unusually large intestinal lipid droplet stores throughout their life[30-33].
64 Accordingly, redistributing lipids intended for secreted lipoproteins to intestinal lipid droplets is
65 sufficient to extend lifespan[29]. However, in long-lived animals, it is unclear whether adult intestinal
66 lipid stores are simply a consequence of reduced demand from the germline[34], a long-term energy
67 store rationing strategy[35] or a more direct mediator of somatic maintenance. Here, while
68 identifying the regulatory network of SQST-1, we found that lipid droplet accumulation in long-
69 lived nematodes represents a novel proteostatic mechanism that reduces overall SQST-1 and
70 ubiquitination levels, and mitigates age-related proteostatic stress.
71
72 **RESULTS**
73 *SQST-1 over-expression is detrimental to lifespan in C. elegans*
74 We initially considered the possibility that increasing SQST-1 may improve proteostasis by
75 enhancing the ability of cells to mediate selective autophagy. We hypothesized that increasing
76 the expression of a receptor that recognizes ubiquitinated cargoes may suffice in driving their
77 degradation. While this study was being conducted, the Hansen laboratory showed that over-
78 expressing SQST-1 can extend lifespan at 20°C[16]. Since longevity interventions and temperature

79 mechanistically interact[36], we examined lifespan at both 20°C and 25°C using several over-
80 expressing strains (*psqst-1::sqst-1::rfp*, *psqst-1::sqst-1::gfp::rfp*), including two created in the
81 Hansen laboratory (*psqst-1::sqst-1::gfp* and *psqst-1::sqst-1*)[16]. Over-expression of SQST-1 was
82 unexpectedly detrimental at 25°C (**Figure 1a-c, Supplemental Figure 1a-c**) and was not
83 sufficient to extend lifespan at 20°C (**Figure 1d-f**). While our findings at 20°C differ from recent
84 literature[16], highlighting potential lab-to-lab experimental variations, our findings are in line with
85 most studies about the autophagy pathway and aging, i.e. that over-expressing an autophagy
86 receptor might not necessarily be sufficient to improve lifespan[37]. At 25°C, SQST-1 clearly
87 accumulates in the head, as well as the gonadal and intestinal tissues (**Supplemental Figure 1d**)
88 as previously reported[38]. A closer investigation into the temperature-dependent differences in
89 lifespan revealed marked upregulation of *sqst-1* mRNA at higher temperature in these strains
90 (from ~5-fold in wild-type, up to ~75 fold in SQST-1::GFP over-expressing animals) (**Figure 1g**).
91 In order to measure the active trafficking of SQST-1 into the lysosome as a guide for selective
92 autophagy, we developed a tandem reporter system expressing SQST-1 fused to both GFP and
93 RFP[7] (GFP signal is quenched in low pH environments). We confirmed that the conversion of
94 tandem SQST-1 into an RFP-only signal is reduced in *lgg-1*- or *lgg-2*-silenced animals
95 (**Supplemental Figure 1e**). and autophagy-deficient *atg-18* mutants (**Supplemental Figure 1f**).
96 While relatively modest at 20°C (**Figure 1h-i**), increasing temperature up to 30°C for 24 hours
97 significantly enhanced the conversion to the RFP-only SQST-1 signal in the SQST-1 tandem
98 reporter, suggesting that selective autophagy is induced with heat stress. Substantial
99 temperature-dependent intestinal and neuronal accumulation of SQST-1 occurred during aging
100 and over-expressing SQST-1 at 25°C was also accompanied by higher levels of total ubiquitinated
101 proteins (**Figure 1a-f inset and Supplemental Figure 1g-h**). While over-expressing SQST-1 was
102 detrimental at 25°C, so was the loss of *sqst-1* (**Supplemental Figure 1i-j**), suggesting that SQST-
103 1 function has a temperature-specific role in the lifespan of wild-type animals. Expression and

104 steady-state levels of SQST-1 likely need to be tightly coordinated with cargo targeting and more
105 importantly, with the rate of protein degradation systems (i.e. autophagy and proteasome).
106 Altogether, we found that solely increasing SQST-1 is detrimental for lifespan at 25°C and
107 inconsequential at 20°C, indicating a temperature-dependent effect on SQST-1 dynamics in
108 aging.
109
110 *Proteins that bind lipid droplets modulate SQST-1 dynamics*
111 In order to better understand how SQST-1 is regulated, we opted for an unbiased genome-wide
112 RNAi screening approach in an integrated SQST-1 over-expressing strain (*psqst-1::sqst-1::gfp*)
113 at 25°C during development. SQST-1 modulators were subsequently validated by gene silencing
114 in a separate over-expressing strain (*psqst-1::sqst-1::rfp*) during development and adulthood.
115 Interestingly, the vast majority of modifiers led to the intestinal accumulation of fluorescently
116 tagged SQST-1 in both development and adulthood; no modifiers were identified that consistently
117 caused decreased levels of SQST-1 (**Supplemental Table 1**). A substantial portion of genetic
118 modifiers clustered in ribosomal-related proteins, including proteins coding for small and large
119 subunits, suggesting that ribosomal assembly and function substantially impact SQST-1
120 dynamics (**Figure 2a**, **Supplemental Table 1**). This is in line with studies in *C. elegans*[2] and
121 killifish[39], highlighting the age-related instability of several ribosomal proteins and consequent
122 ribosomal mis-assembly. Loss of ribosome subunit RPL-43 was also found to increase SQST-1
123 accumulation during development[40]. Since SQSTM1 was also recently reported to associated
124 with lipid droplets in macrophages[41], we wondered if SQST-1 might also associate with lipid
125 droplets. We co-expressed SQST-1::RFP and the lipid resident protein DHS-3 fused to GFP [42] in
126 nematodes and we found that close to 50% of SQST-1::RFP localizes to lipid droplets when
127 autophagy is inhibited (**Figure 2b and Supplemental Figure 2a**). Thus, we investigated whether
128 SQST-1 modulators may also be related to lipid droplet metabolism. We compared our SQST-1

129 modulators to proteins that have been found to bind lipid droplets[43] and found significant overlap
130 (p < 5.745e-60) (**Figure 2c**). Interestingly, several proteins prone to age-dependent aggregation[2]
131 also modulated SQST-1 accumulation (p < 6.030e-10) (**Figure 2c**). Overall, 17 SQST-1
132 modulators have the propensity to both aggregate with age and bind lipid droplets (**Figure 2c,**
133 **Supplemental Table 2)**. Several ribosomal subunits (*rps* and *rpl* genes) and mRNA-related
134 proteins (*inf-1* and *pab-1*) emerged, along with the HSP70 chaperone family member *hsp-*
135 *1/HSPA8*, indicating that ribosomal assembly, translation initiation, and protein folding are
136 important regulators of SQST-1 dynamics (**Figure 2d**). SQST-1::RFP accumulation upon
137 silencing of these modifiers was mostly gonadal and intestinal (**Figure 2d, Supplemental Figure**
138 **2b**). Interestingly, the expression of *sqst-1* was differentially regulated by the 17 SQST-1
139 modulators whereas silencing large ribosomal proteins generally increased *sqst-1* expression
140 (**Supplemental Figure 2b**). This highlights that *sqst-1* expression is potentially sensitive to
141 ribosomal protein stoichiometry. Here, our comparative analysis suggests that age-related SQST-
142 1 accumulation may be partly attributed to altered interactions between lipid droplets and
143 progressively unstable protein complexes like the ribosome.
144
145 *Elevated lipid droplets reduce SQST-1 accumulation and extend lifespan*
146 Intestinal lipid droplet accumulation is a striking feature of several long-lived nematodes[30-32]. Since
147 SQST-1 accumulated on lipid droplets when autophagy was inhibited (**Figure 2b**), and several
148 SQST-1 modifiers bind lipid droplets (**Figure 2c**), we speculated that lipid droplets may underlie
149 the ability of long-lived animals to stabilize or facilitate clearance of potentially aggregating
150 proteins and maintain proteome stability during aging. In order to specifically stimulate intestinal
151 lipid droplet accumulation and expansion, we silenced the conserved cytosolic lipase *atgl-1/ATGL*
152 [44] during adulthood to attenuate lipid droplet breakdown, which led to larger lipid stores thereby
153 mimicking a key feature of several long-lived animals (**Figure 3a, inset**). Silencing *atgl-1* resulted
154 in a significant lifespan extension in wild-type animals (12-28%), indicating that lipid droplet

155 accumulation is sufficient to mediate longevity (**Figure 3a-b**). Silencing ATGL-1 activator *lid-1* or
156 hormone-sensitive lipase orthologue *hosl-1*[45] also led to significant reduction in SQST-1
157 accumulation (**Supplemental Figure 2c**). These observations pointed to a possible lipid droplet-
158 mediated cytoprotective mechanism[46]. Indeed, silencing *atgl-1* in SQST-1::RFP over-expressing
159 animals led to a substantial increase in lifespan (**Figure 3c)** accompanied by a marked decrease
160 in SQST-1 accumulation (**Figure 3d**). Similar observations were made in animals over-expressing
161 SQST-1::GFP (**Supplemental Figure 2d**), suggesting that the lipid droplet-mediated effects
162 impacts SQST-1-mediated selective autophagy.
163 To determine whether accumulation of lipids is able to improve the lifespan of proteostatically-
164 impaired mutants, we silenced *atgl-1* in three well-established short-lived mutants, including *daf-*
165 *16(mu86)*, *hlh-30(tm1978),* and *hsf-1(sy441)*[47]. Notably, the expression of these transcription
166 factors was increased at 25°C compared to 20°C, suggesting that their function may be stimulated
167 by heat (**Supplemental Figure 2e**). Silencing *atgl-1* extended the lifespan of *daf-16* and *hlh-30*
168 mutants, but not the lifespan of *hsf-1* mutants (**Figure 3e-g**), indicating that lipid droplet-mediated
169 lifespan extension may require the expression of key chaperones regulated by HSF-1/HSF1, such
170 as heat shock protein HSP-1, which binds lipid droplets and modulates SQST-1 levels (**Figure**
171 **2d**). Interestingly, lipid droplets may harbor chaperones with roles in aggregate clearance[48].
172 Notably, autophagic activity, as measured by the tandem mCherry::GFP::LGG-1 reporter[7],
173 showed that *atgl-1* silencing increases the conversion of autophagosomes (GFP+mCherry -
174 yellow puncta) into autolysosomes (mCherry only - red puncta) (**Figure 3h, Supplemental Figure**
175 **2f**). Accordingly, the lifespan of autophagy-deficient *atg-7* mutants was not increased by silencing
176 *atgl-1* (**Supplemental Figure 2g**).
177 As our lifespan analyses highlighted novel proteostatic and longevity roles for lipid droplets, we
178 reasoned that long-lived animals with large lipid stores should accumulate less intestinal SQST-
179 1. Strikingly, *daf-2(e1370)* expressing SQST-1::GFP (**Figure 3i**) or SQST-1::RFP (**Supplemental**
180 **Figure 2h**) accumulated negligible intestinal SQST-1 during aging (GFP signal in mid-section was

181 entirely gonadal, see wild-type comparison in **Figure 1b**). In addition, SQST-1 over-expression
182 did not significantly affect the long lifespan of *daf-2* animals (**Figure 3i**). Loss of *sqst-1* did not
183 affect the lifespan of *daf-2* animals (**Supplemental Figure 2i**), as previously shown[16], highlighting
184 that SQST-1 function becomes less important at 25°C for the lifespan of organisms with relatively
185 stable proteomes and high lipid stores. The extent of heat-induced increase in SQST-1-mediated
186 selective autophagy was also attenuated in *daf-2* animals (**Supplemental Figure 2j**) compared
187 to wild-type (**Figure 1h**), suggesting that elevated lipid droplets may buffer the need for SQST-1
188 function during heat stress. Silencing *atgl-1* in *daf-2* animals enhanced their intestinal lipid stores
189 and further extended their lifespan (**Figure 3j**), indicating that elevated lipid droplet accumulation
190 can also extend lifespan in animals with enhanced proteostasis. Altogether, our data present an
191 important and previously unrecognized role for lipid droplets in SQST-1 dynamics and longevity.
192
193 *Silencing atgl-1 elicits limited changes in gene expression*
194 Lipid droplets have been recently shown to coordinate transcriptional programs by sequestering
195 factors that modulate transcription[49]. Since HSF-1 was required for lifespan extension by *atgl-1*
196 silencing, we hypothesized that the lipid droplet increase associated with *atgl-1* silencing might
197 affect the expression of HSF-1-regulated targets. Using RNA sequencing (RNA-seq), we found
198 that enhancing lipid stores by silencing *atgl-1* in WT or *daf-2* animals had limited effect on global
199 transcription. Silencing *atgl-1* resulted in 13 overlapping differentially expressed genes (DEG) in
200 wild-type animals and *daf-2* mutants of which 7 genes are down-regulated in both cases
201 (**Supplemental Figure 3a-b**). The mRNA levels of *sqst-1* remained unchanged by *atgl-1* silencing
202 (**Supplemental Figure 3c**). Altering *atgl-1* levels (silencing or over-expression) led to differential
203 expression of 50 overlapping genes, with no discernable transcription factor signature
204 (**Supplemental Figure 3d-e**). In addition, expression of *sqst-1* was unchanged in wild-type
205 animals with low or high levels of *atgl-1* (**Supplemental Figure 3e**). Overall, we concluded that
206 transcriptional regulation may not contribute significantly to the proteostatic-enhancing and

207 lifespan-extending effects of lipid droplets. Therefore, lipid droplets may impact proteostasis via
208 a more direct mechanism on the proteome itself.
209
210 *Lipid droplets enhance proteostasis by modulating the accumulation of ubiquitinated proteins*
211 The emerging connection between lipid droplet stores and proteome stability led us to investigate
212 how lipid droplet loss affects proteostasis and SQST-1 abundance. First, we tested whether lipid
213 droplet depletion affects lifespan using ATGL-1::GFP over-expressing animals[50]. Unlike at 20°C
214 (**Supplemental Table 3**)[51], we found that over-expressing ATGL-1 was detrimental to lifespan at
215 25°C (**Figure 4a**) and led to a significant increase in SQST-1 intestinal accumulation
216 accompanied by lower lipid stores (**Figure 4b**), suggesting that loss of lipid droplet stores can
217 interfere with SQST-1 dynamics. When autophagy or proteasome function was reduced by
218 silencing autophagosome protein *lgg-1* or proteasome subunit *rpn-6.1*, respectively, ubiquitinated
219 protein levels were higher in animals with lower lipid stores, suggesting that lipid droplets may
220 buffer the proteome and facilitate the processing of unstable or misfolded proteins (**Figure 4c**).
221 Strikingly, analyzing lipid droplets revealed preferential accumulation of ubiquitinated proteins in
222 lipid droplet-enriched fractions (**Figure 4d, Supplemental Figure 4a**), indicating that lipid droplets
223 contain a significant amount of proteins bound for degradation. Lipid droplet-associated
224 accumulation of ubiquitinated proteins was increased when autophagic or proteasomal
225 degradation was reduced (**Figure 4d**), suggesting that lipid droplets have the capacity to harbor
226 many degradation cargoes, which may become particularly relevant for proteostasis when
227 autophagic and proteasomal systems are failing during aging.
228 The association and function of ATGL-1 with lipid droplets was recently found to be antagonized
229 by the AAA-ATPase CDC-48/VCP[52]. CDC-48/VCP is best known for its role in ER-associated
230 degradation machinery[53], but it has been associated with other functions including endocytosis[54]
231 and more recently autophagy itself[55]. CDC-48/VCP helps unfold unstable, ubiquitinated, and

232 proteasomal degradation-bound proteins in concert with heat shock protein HSP-70, a key
233 regulated target of HSF-1[56]. Thus, we assayed the effect of the loss of CDC-48 on SQST-1 and
234 ATGL-1 levels using fluorescent reporters. Silencing *cdc-48.2* increased the levels of ATGL-
235 1::GFP (**Supplemental Figure 4b)** and led to the accumulation of SQST-1::RFP (**Supplemental**
236 **Figure 4c**). In mammalian cells, loss of proteasome function drives SQSTM1 to divert cargo to
237 selective autophagy[57], but stimulating proteasomal processing by over-expressing of VCP can
238 reduce SQSTM1 accumulation[58]. Here, we reasoned that CDC-48 functions related to processing
239 ubiquitinated targets and autophagy may underlie the ability of nematodes with elevated lipid
240 droplets to attenuate SQST-1 accumulation and modulate lifespan. Accordingly, silencing *atgl-1*
241 in *cdc-48.1* or *cdc-48.2* mutants failed to significantly extend lifespan (**Supplemental Figure 4d,**
242 **Supplemental Table 4**), indicating that lipid droplet-mediated lifespan extension requires
243 functional CDC-48.
244 As lipid droplet size increases, its surface also increases, and it is possible that the capacity of
245 this organelle to bind and stabilize proteins may also increase as well. Enhancing lipid droplet
246 stores by silencing *atgl-1* reduced the overall accumulation of ubiquitinated proteins, in particular
247 in the lower solubility (5% SDS soluble) fraction (**Figure 4e**), suggesting that typically insoluble
248 proteins are less likely to be ubiquitinated when lipid droplets abound. Notably, the types of
249 proteins that aggregate with age differ between wild-type and long-lived *daf-2* mutants, as the
250 latter tends to accumulate aggregating proteins that are less hydrophobic than those aggregating
251 in wild-type animals[4]. Reducing lipid droplet stores genetically by silencing lipogenic genes *sbp-*
252 *1(SREBP2)*, *lpin-1(LIPN1)* or *fasn-1(FASN)* enhanced SQST-1 accumulation in wild-type animals
253 (**Supplemental Figure 4e**). Similarly, loss of lipid droplet stores by silencing *lpin-1* in *daf-2*
254 resulted in increased SQST-1 accumulation and overall protein ubiquitination (**Figure 4f-g**). As
255 proteostasis failure is a feature of neurodegeneration, we tested the effect of increasing lipid
256 droplet levels in proteotoxic contexts. Animals intestinally-expressing an aggregating poly-
257 glutamine protein fused to YFP (Q44::YFP)[59] had reduced numbers of aggregates when *atgl-1*

258 was silenced **(Figure 4h)**. Reducing the expression of *atgl-1* in a muscle-expressing proteotoxic
259 amyloid protein Aβ-42 resulted in a marked protection against aggregation-associated paralysis[60]
260 (**Figure 4i**). Altogether, our data demonstrate that lipid droplets are important for proteostasis and
261 contribute to lifespan by facilitating autophagy and stabilizing the proteome.
262

263 **DISCUSSION**

264 Decades of aging research has uncovered key longevity-regulating pathways in *C. elegans*[47], yet
265 the role of lipid droplets in the lifespan of several established long-lived nematodes has remained
266 unresolved. Here, while studying the regulation of the selective autophagy receptor SQST-1, we
267 unexpectedly uncovered a direct role for lipid droplets in proteostasis and lifespan. Several SQST-
268 1 modulators associate with lipid droplets and aggregate with age, including ribosomal,
269 translation-related, and folding-related proteins[43]. Ribosomal assembly dysfunction due to loss in
270 subunit stoichiometry may burden the autophagy machinery, and contribute to age-related
271 proteotoxicity[39]. Importantly, lipid droplet accumulation, by silencing cytosolic triacylglycerol lipase
272 *atgl-1/ATGL,* mitigates the progressive age-related SQST-1 accumulation, a benefit recapitulated
273 in long-lived, lipid droplet-rich *daf-2* mutant animals. Lipid droplets are cytoprotective as they
274 prevent aberrant SQST-1 accumulation, in part via the functioning of AAA-ATPase CDC-48/VCP
275 which processes ubiquitinated proteins for proteasomal degradation[61]. Strikingly, we found that
276 the majority of soluble ubiquitinated proteins in nematodes was associated with lipid droplets,
277 suggesting that unstable proteins bound for degradation may be stabilized by the surface of lipid
278 droplets. Our findings also provide support to the importance of the emerging lipid-droplet-
279 mediated protein degradation process[62,63] in longevity and aging. Altogether, our study
280 strengthens the emerging concept that lipid droplets serve as a buffer for proteostasis[46] by
281 stabilizing proteomes and coordinating protein degradation machineries.
282 Understanding the regulation of SQST-1/SQSTM1 during aging and in different disease contexts
283 is important in order to determine the validity of stimulating selective autophagy as a therapeutic

284 strategy to improve proteostasis in age-related diseases[64]. Here, we find that over-expressing
285 SQST-1 had no effect on the lifespan of wild-type animals at 20°C[16] whereas elevated SQST-1
286 level at 25°C was detrimental. In hindsight, one may have predicted that over-expressing a
287 ubiquitin-binding protein with a propensity for oligomerization[65] might not be necessarily
288 advantageous, particularly in organisms nearing their protein solubility limit[2,3] and displaying
289 overall proteome instability during aging[5]. SQST-1 over-expression was primarily visible in
290 neuronal, gonadal and intestinal cells and accumulated in a temperature-dependent manner and
291 progressively during aging. The inability of stressed and aging animals to process ubiquitinated
292 cargos bound for proteasomal or autophagic degradation may lead to a gradual build-up of SQST-
293 1. Accordingly, SQST-1 over-expression may over-sensitize the animals to unstable,
294 ubiquitination-prone proteins, posing an additional challenge to the autophagic machinery. This
295 is exemplified by recent evidence that reducing SQST-1 specifically in the neurons of a nematode
296 model of ALS is protective[66], possibly since mutant fused in sarcoma (FUS) expression promotes
297 SQST-1 accumulation, which exacerbates proteotoxicity and neurodegeneration. Notably,
298 SQSTM1 can phase separate when interacting with ubiquitinated cargoes[67], but the impact of the
299 formation of these condensates on overall proteostasis is unclear.
300 Lipid droplet accumulation is a prominent and under-explored phenotype of several long-lived
301 nematodes, including well-established models such as germline-less *glp-1* animals, protein
302 translation *rsks-1* mutants, insulin/IGF-1 receptor *daf-2* mutants[68] as well as in long-lived animals
303 with reduced nuclear export[69]. In addition, lifespan extension by inhibiting intestinal lipid secretion
304 mediated by vitellogenins results in lipid redistribution to intestinal lipid droplet stores[29], a process
305 believed to generate precursors for lysosomally-derived lipid signals[28]. While enhanced lysosomal
306 lipolysis and lipophagy may stimulate longevity-associated lipid signaling, overactive cytosolic
307 lipolysis decreases the ability of cells to maintain a stable proteome, which may burden the
308 selective autophagy machinery. Our findings support that lipid droplets are much more than just

309 lipid storage organelles[46] and can serve as interfaces to enable protein stabilization and
310 processing.
311 Rationing of intestinal lipid stores was originally evoked as a potential mechanism to provide long-
312 term energy for dauer larvae that arrest feeding[35]. Here, we propose a role for lipid stores during
313 adulthood that focuses on their capacity to buffer proteostasis during aging in concert with heat
314 shock chaperones, thereby unburdening protein degradation systems (**Figure 5**). ATGL-1 over-
315 expression leads to lipid store depletion [51], but, more importantly, it also removes the protection
316 conferred by lipid droplets and renders animals vulnerable to proteotoxic stress associated with
317 reduced proteasomal function, heat and aging. Thus, regulating the activity of ATGL-1 via
318 transcription[70], post-translational modification[71] or alteration in CDC48/VCP activity[52] provide a
319 mechanism by which cells modify protein homeostasis. Overall, our data also show that the lipid
320 droplet-mediated decrease in protein ubiquitination and the enhancement in lifespan require the
321 function of the AAA-ATPase CDC-48/VCP, a ubiquitin protein processing enzyme and autophagy
322 modulator[55].
323 Lipid droplet expansion may belong to an arsenal of proteostatic measures that lipid-storing cells
324 and possibly neurons can employ to prevent protein misfolding and aggregation. While lipid
325 droplet accumulation in immune cells such as macrophages[72] and microglia[73] may be
326 inflammatory and contribute to aging, lipid droplets may confer some post-mitotic, differentiated
327 cells with added protection against protein aggregation[48] and mitochondrial lipid overload[74]. For
328 example, lipid droplet accumulation in Alzheimer's disease pathogenesis[75] may highlight an effort
329 from neuronal cells to improve proteome stability and resilience against progressive
330 proteotoxicity. Notably, drastic inhibition of triacylglycerol lipolysis becomes detrimental to
331 neurons[76] as larger lipid droplets are less easily broken down[50]. However, a recent study showed
332 that lipid droplet accumulation protected hyper-activated neurons from cell death[77], a
333 phenomenon potentially relevant in Alzheimer's disease[78]. Thus, moderate accumulation of lipid
334 droplets may be more desirable to provide protection against age-related proteotoxicity. In

335 agreement, our data show marked protection against paralysis in a proteostatic Alzheimer's
336 disease model by attenuating cytosolic lipolysis.
337 Enhancing proteostasis by stimulating the autophagy process has emerged as an attractive
338 strategy to mitigate several age-related diseases with pathological proteostatic decline such as
339 neurodegenerative diseases [79]. However, our study indicates that stimulating selective autophagy
340 by specifically increasing the expression of one selective autophagy receptor, SQST-1/SQSTM1,
341 is not sufficient to improve proteostasis and may exacerbate age-related proteostatic collapse.
342 Overall, our study suggests that therapeutic improvement in proteostasis may benefit from a
343 combinatorial approach in which the whole autophagy/lysosomal machinery is stimulated
344 concomitantly with a modest reduction in lipid droplet breakdown. Such an approach may prevent
345 pathogenic burdening of the autophagy/lysosome pathway with cargoes that could have
346 otherwise been stabilized by lipid droplets or routed to the proteasome.
347

348 **METHODS**

349 ***C. elegans* strain maintenance**

350 Nematodes were maintained at 20°C on agar NGM plates seeded with OP50 *E. coli* unless
351 otherwise noted, as previously described[80]. Synchronized populations were prepared using a
352 sodium hypochlorite solution to collect eggs as previously described[81]. Supplemental Tables 5
353 and 6 contains the list of strains used in this study. HT115 *E. coli* and RNAi clones from the
354 Ahringer library (Source Bioscience) were used for RNAi experiments[82].
355

356 **Transgenic strain construction**

357 DNA constructs for the plasmids pLAP26 (*psqst-1::sqst-1::rfp::unc-54 3'UTR*) and pLAP29 (*psqst-*
358 *1::sqst-1::gfp::rfp::unc-54 3'UTR*) were assembled using HiFi cloning and were injected into the
359 germline of Day 1 adults (pLAP26 was co-injected with the pLAP7 (*myo-2::gfp::unc-54)*).
360 Transgenic progeny was UV-irradiated for extrachromosomal array integration and selected for

361 100% transmission rate and backcrossed at least four times to wildtype N2. Details about strain
362 construction are provided in Supplemental Table 6.
363
364 **Genome-wide RNAi screen**
365 Approximately 50 synchronized transgenic eggs (*psqst-1::SQST-1::GFP*) were transferred onto
366 plates seeded with RNAi against all genes from the Ahringer library (Source BioScience), which
367 represents about 86% of the predicted genes in the *C. elegans* genome[82]. Nematodes were
368 developed at 25°C and changes in GFP intensity or expression pattern were monitored on Day 1
369 of adulthood. As a negative control, bacteria expressing the L4440 backbone (i.e. empty vector)
370 expressed in HT115 *E. coli* were used. The identity of each RNAi was not known to the scorer
371 and fluorescence intensity was scored using a V20 dissection fluorescence microscope (Zeiss).
372 Modifiers from the genome-wide RNAi screen were sequenced (GENEWIZ), validated three times
373 and corroborated using transgenic animals expressing *SQST-1::RFP*. RNAi against the genes
374 with the strongest effect on GFP expression were subsequently validated by silencing in
375 adulthood only. Details are provided in Supplemental Tables 1 and 2.
376
377 **Lifespan analyses**
378 Eggs obtained from bleaching were transferred onto OP50 *E. coli.* bacteria-seeded agar plates.
379 All lifespan analyses were carried out at 25°C starting at Day 1 of adulthood after development at
380 20°C, unless otherwise noted. For gene knockdown experiments, worms were transferred to
381 control bacteria expressing the empty vector (L4440) or expressing corresponding RNAi at day
382 one of adulthood. Viability was scored every 1 to 3 days, as previously described[83]. Survival
383 curves and statistical analysis were generated using the Stata 15.0 software (StataCorp). Details
384 are provided in Supplemental Tables 3 and 4.
385
386 **Comparative analyses**

387 Knocked-down genes with the strongest effect on SQST-1::GFP levels were analyzed for gene
388 ontology using WormCat[84] to identify which pathways were enriched. RNAi against genes that
389 overlapped with the SQST-1 modulators, lipid droplet proteome[43], and insoluble proteins[2] were
390 then tested in adult-only experiments. Statistical significance of the overlap between any two
391 groups of genes was calculated by hypergeometric probability (nemates.org, Lund laboratory,
392 University of Kentucky). For adult-only RNAi validation, eggs from wild-type and SQST-1
393 transgenic animals were developed on OP50 *E coli.* bacteria at 20°C and transferred to
394 corresponding RNAi plates at Day 1 of adulthood and grown at 25°C for an additional 72 hours.
395 Adults were transferred away from their progeny and bright field and fluorescent images were
396 taken daily.
397
398 **Imaging and analyses**
399 Worms were visualized using a Zeiss Discovery V20 fluorescence dissecting microscope (Zeiss,
400 White Plains, NY). Worms were immobilized with 0.1% sodium azide in M9 solution (42 mM
401 Na2HPO4 22 mM KH2PO4 86 mM NaCl, 1 mM MgSO4-7H2O) on agar plates and images were
402 taken via Zen imaging software, using consistent parameters (magnification and exposure)
403 within each experiment. For quantification of fluorescent signal, total fluorescence of each worm
404 in each image was analyzed using ImageJ software and averaged for mean total fluorescence.
405 Confocal microscopy images were obtained on an Olympus FV3000 inverted confocal laser
406 scanning microscope (Leduc Bioimaging Facility, Brown University). Quantification of
407 autophagosomes marked by GFP and mCherry showing yellow puncta and autolysosomes
408 marked with only mCherry as GFP is quenched in acidic pH showing up as red puncta in the
409 LGG-1 tandem reporter strain was carried out by color thresholding composite images for yellow
410 or red puncta followed by counting the thresholded puncta using particle analysis on ImageJ.
411 The overlap between lipid droplet protein (DHS-3) and tagged SQST-1 in the over-expressing

412 strain was also performed using color thresholding followed by particle analysis functions in
413 ImageJ (NIH).
414
415 **Lipid staining**
416 Worms were collected and washed twice with M9 solution and then fixed with 60% isopropanol
417 for 30 minutes. After fixation, worms were stained overnight on a rocker with freshly prepared
418 60% Oil Red O (stock solution of 0.5% ORO in isopropanol diluted with water, equilibrated
419 overnight on a rocker, and gravity-filtered). The following day, worms were washed with TBS-T
420 (50 mM Tris base, 150 mM Tris HCl, 1.5 M NaCl, and 0.05% Tween-20) and imaged using a
421 Zeiss Discovery V20 fluorescence dissecting microscope.
422
423 **Gene expression analysis**
424 RNA was extracted from approximately 3,000 Day 1 worms and cDNA was prepared as
425 previously described [8]. Gene expression levels were measured in biological triplicates using iTaq
426 Universal SYBR Green Supermix (BIO-RAD), and a Roche LightCycler 96 (Indianapolis, IN).
427 Expression was normalized using 2 housekeeping genes, *act-1* and *cyn-1* and statistical analyses
428 were performed using GraphPad Prism 7 (GraphPad Software). See Supplemental Table 7 for
429 qPCR primers details.
430
431 **RNAseq sample preparation and analysis**
432 WT or *daf-2* mutant worms were developed on OP50 at 20°C and transferred to corresponding
433 RNAi plates at Day 1 of adulthood and grown at 25°C for an additional 96 hours. Worms over-
434 expressing ATGL-1::GFP were developed on OP50 at 20°C and grown at 25°C for an additional
435 96 hours. Adults were transferred away from their progeny daily. RNA was extracted and cDNA
436 was prepared as previously described[8]. RNA quality was confirmed by BioAnalyzer (Genomics

437 Core, Brown University), and *atgl-1* silencing was confirmed by qPCR before submitting samples
438 for RNAseq analysis by GENEWIZ as previously described[8].
439
440 **Lipid droplet fractionation**
441 Lipid droplets were isolated by ultracentrifugation from 24,000 Day 5 animals grown at 25°C on
442 RNAi for 96 hours. Worms were homogenized with a ball-bearing homogenizer in MSB buffer
443 (250mM sucrose and 10mM Tris-HCl pH 7.4) containing protease inhibitor (Roche). The lysate
444 was cleared of cuticle debris and unlysed worms by centrifuging at 500 x g for 5 minutes. 10% of
445 the cleared lysate was reserved as "Input". Nuclei and non-lipid droplet organelles were pelleted
446 out of the cytosol by an ultracentrifugation spin at 45,000 RPM in a TLA100.1 rotor for 30 minutes
447 at 4°C. The lipid droplet layer at the top of the centrifugation tube was aspirated, and
448 contaminating organelles were removed by an additional centrifugation of the lipid droplet fraction.
449 The final volume of lipid droplet and cytosol fractions were kept consistent across conditions.
450
451 **Immunoblotting**
452 Protein lysates were collected from worms using RIPA buffer (50 mM Tris-HCl, 250 mM sucrose,
453 1 mM EDTA, and Roche protease inhibitor tablet, with 1% or 5% SDS) and a handheld
454 homogenizer, and cleared lysate protein concentrations were quantified using the DC Protein
455 Assay kit (BIO-RAD). Equal amounts of total protein (10 μg) or comparative volumes for lipid
456 droplet fractions (Input volume is 10% of lipid droplet and cytosol fractions) were separated by
457 SDS-PAGE on a 4-15% Tris-Glycine gel and transferred to nitrocellulose. The membrane was
458 briefly stained with Ponceau S to confirm even transfer, rinsed with TBS-T until clear, blocked
459 with 5% nonfat dry milk in TBS-T, and immunoblotted with anti-Ubiquitin (Invitrogen MAI-10035),
460 anti-GFP (Santa Cruz SC-8334), and anti-Actin (Milllipore, MAB1501R). The membrane was
461 developed using SuperSignal West Femto Maximum Sensitivity Substrate (ThermoFisher) and
462 imaged on a ChemiDoc Imaging System (BIO-RAD).

463

464 **DATA AVAILABILITY STATEMENT**

465 RNA sequencing data are accessible on NCBI GEO (Accession number: GEO204953).

466

467 **CONTRIBUTIONS**

468 AVK, JM, WMP and JAL performed lifespan analyses and imaging as well as RNAi sequencing,
469 validation, and analysis. AVK, JM, JAL and JRJ validated the whole-genome RNAi screening. JM
470 performed the RNA sequencing and lipid droplet analyses. WMP conducted lipid staining and
471 AVK performed the confocal microscopy imaging. DIR performed RNAi sequencing and
472 conducted qPCR analyses. CN, RP and JLA performed lifespan analysis repeats. SQW and WMP
473 developed SQST-1 over-expressing and tandem reporter strains. LRL designed the experiments,
474 conducted initial RNAi screening, imaging, qPCR and lifespan analyses, and wrote the
475 manuscript. All co-authors edited the manuscript.

476

477 **ACKNOWLEDGEMENTS**

478 We are grateful for the technical support provided by Erin McConnell, Rachel Tam and Tuong
479 Tran. We thank the Malene Hansen laboratory (SBPMDI) and the Caenorhabditis Genetics
480 Center (U. Minnesota, P40 OD010440) for providing transgenic and mutant strains and the
481 Andrew Dillin laboratory (UC Berkeley/HHMI) for sharing expression plasmids. This work was
482 funded by grants from the National Institute of Health (R00 AG042494, R01 AG051810 and R21
483 AG068922) and a Glenn Award for Research in Biological Mechanisms of Aging from the Glenn
484 Foundation for Medical Research to LRL.

485

486 **REFERENCES**

487 1 Koga, H., Kaushik, S. & Cuervo, A. M. Protein homeostasis and aging: The importance of
488 exquisite quality control. *Ageing Res Rev* **10**, 205-215, doi:10.1016/j.arr.2010.02.001
489 (2011).
490 2 Reis-Rodrigues, P. *et al.* Proteomic analysis of age-dependent changes in protein
491 solubility identifies genes that modulate lifespan. *Aging Cell* **11**, 120-127,
492 doi:10.1111/j.1474-9726.2011.00765.x (2012).
493 3 Sui, X. *et al.* Widespread remodeling of proteome solubility in response to different protein
494 homeostasis stresses. *Proc Natl Acad Sci U S A* **117**, 2422-2431,
495 doi:10.1073/pnas.1912897117 (2020).
496 4 Walther, D. M. *et al.* Widespread Proteome Remodeling and Aggregation in Aging C.
497 elegans. *Cell* **161**, 919-932, doi:10.1016/j.cell.2015.03.032 (2015).
498 5 Ben-Zvi, A., Miller, E. A. & Morimoto, R. I. Collapse of proteostasis represents an early
499 molecular event in Caenorhabditis elegans aging. *Proc Natl Acad Sci U S A* **106**, 14914-
500 14919, doi:0902882106 [pii] 10.1073/pnas.0902882106 (2009).
501 6 Vilchez, D. *et al.* RPN-6 determines C. elegans longevity under proteotoxic stress
502 conditions. *Nature* **489**, 263-268, doi:nature11315 [pii] 10.1038/nature11315 (2012).
503 7 Chang, J. T., Kumsta, C., Hellman, A. B., Adams, L. M. & Hansen, M. Spatiotemporal
504 regulation of autophagy during Caenorhabditis elegans aging. *eLife* **6**,
505 doi:10.7554/eLife.18459 (2017).
506 8 Lapierre, L. R. *et al.* The TFEB orthologue HLH-30 regulates autophagy and modulates
507 longevity in Caenorhabditis elegans. *Nat Commun* **4**, 2267, doi:ncomms3267 [pii]
508 10.1038/ncomms3267 (2013).
509 9 Morley, J. F. & Morimoto, R. I. Regulation of longevity in Caenorhabditis elegans by heat
510 shock factor and molecular chaperones. *Mol Biol Cell* **15**, 657-664, doi:10.1091/mbc.E03-
511 07-0532 E03-07-0532 [pii] (2004).

512 10 Tiku, V. *et al.* Small nucleoli are a cellular hallmark of longevity. *Nat Commun* **8**, 16083,
513 doi:10.1038/ncomms16083 (2017).
514 11 Visscher, M. *et al.* Proteome-wide Changes in Protein Turnover Rates in C. elegans
515 Models of Longevity and Age-Related Disease. *Cell Rep* **16**, 3041-3051,
516 doi:10.1016/j.celrep.2016.08.025 (2016).
517 12 Dhondt, I. *et al.* FOXO/DAF-16 Activation Slows Down Turnover of the Majority of Proteins
518 in C. elegans. *Cell Rep* **16**, 3028-3040, doi:10.1016/j.celrep.2016.07.088 (2016).
519 13 Kirkin, V. & Rogov, V. V. A Diversity of Selective Autophagy Receptors Determines the
520 Specificity of the Autophagy Pathway. *Mol Cell* **76**, 268-285,
521 doi:10.1016/j.molcel.2019.09.005 (2019).
522 14 Pankiv, S. *et al.* p62/SQSTM1 binds directly to Atg8/LC3 to facilitate degradation of
523 ubiquitinated protein aggregates by autophagy. *J Biol Chem* **282**, 24131-24145,
524 doi:M702824200 [pii] 10.1074/jbc.M702824200 (2007).
525 15 Aparicio, R., Hansen, M., Walker, D. W. & Kumsta, C. The selective autophagy receptor
526 SQSTM1/p62 improves lifespan and proteostasis in an evolutionarily conserved manner.
527 *Autophagy* **16**, 772-774, doi:10.1080/15548627.2020.1725404 (2020).
528 16 Kumsta, C. *et al.* The autophagy receptor p62/SQST-1 promotes proteostasis and
529 longevity in C. elegans by inducing autophagy. *Nat Commun* **10**, 5648,
530 doi:10.1038/s41467-019-13540-4 (2019).
531 17 Aparicio, R., Rana, A. & Walker, D. W. Upregulation of the Autophagy Adaptor
532 p62/SQSTM1 Prolongs Health and Lifespan in Middle-Aged Drosophila. *Cell Rep* **28**,
533 1029-1040 e1025, doi:10.1016/j.celrep.2019.06.070 (2019).
534 18 Palikaras, K., Lionaki, E. & Tavernarakis, N. Coordination of mitophagy and mitochondrial
535 biogenesis during ageing in C. elegans. *Nature* **521**, 525-528, doi:10.1038/nature14300
536 (2015).

537 19 Johansen, T. & Lamark, T. Selective autophagy mediated by autophagic adapter proteins.
538 *Autophagy* **7**, 279-296, doi:14487 [pii] (2011).
539 20 Zhang, B. *et al.* Brain-gut communications via distinct neuroendocrine signals
540 bidirectionally regulate longevity in C. elegans. *Genes Dev* **32**, 258-270,
541 doi:10.1101/gad.309625.117 (2018).
542 21 Antebi, A. Regulation of longevity by the reproductive system. *Exp Gerontol* **48**, 596-602,
543 doi:10.1016/j.exger.2012.09.009 (2013).
544 22 Gelino, S. *et al.* Intestinal Autophagy Improves Healthspan and Longevity in C. elegans
545 during Dietary Restriction. *PLoS Genet* **12**, e1006135, doi:10.1371/journal.pgen.1006135
546 (2016).
547 23 Lapierre, L. R., Gelino, S., Melendez, A. & Hansen, M. Autophagy and lipid metabolism
548 coordinately modulate life span in germline-less C. elegans. *Curr Biol* **21**, 1507-1514,
549 doi:S0960-9822(11)00844-X [pii] 10.1016/j.cub.2011.07.042 (2011).
550 24 Wang, M. C., O'Rourke, E. J. & Ruvkun, G. Fat metabolism links germline stem cells and
551 longevity in C. elegans. *Science* **322**, 957-960, doi:322/5903/957 [pii]
552 10.1126/science.1162011 (2008).
553 25 Lapierre, L. R., Melendez, A. & Hansen, M. Autophagy links lipid metabolism to longevity
554 in C. elegans. *Autophagy* **8**, 144-146, doi:18722 [pii] 10.4161/auto.8.1.18722 (2012).
555 26 Chapin, H. C., Okada, M., Merz, A. J. & Miller, D. L. Tissue-specific autophagy responses
556 to aging and stress in C. elegans. *Aging (Albany NY)* **7**, 419-434 (2015).
557 27 Ramachandran, P. V. *et al.* Lysosomal Signaling Promotes Longevity by Adjusting
558 Mitochondrial Activity. *Dev Cell* **48**, 685-696 e685, doi:10.1016/j.devcel.2018.12.022
559 (2019).
560 28 Folick, A. *et al.* Aging. Lysosomal signaling molecules regulate longevity in Caenorhabditis
561 elegans. *Science* **347**, 83-86, doi:10.1126/science.1258857 (2015).

562 29 Seah, N. E. *et al.* Autophagy-mediated longevity is modulated by lipoprotein biogenesis.
563 *Autophagy* **12**, 261-272, doi:10.1080/15548627.2015.1127464 (2016).
564 30 O'Rourke, E. J., Soukas, A. A., Carr, C. E. & Ruvkun, G. C. elegans major fats are stored
565 in vesicles distinct from lysosome-related organelles. *Cell Metab* **10**, 430-435, doi:S1550-
566 4131(09)00301-5 [pii] 10.1016/j.cmet.2009.10.002 (2009).
567 31 Lapierre, L. R. *et al.* Autophagy genes are required for normal lipid levels in C. elegans.
568 *Autophagy* **9**, 278-286, doi:22930 [pii] 10.4161/auto.22930 (2013).
569 32 Brooks, K. K., Liang, B. & Watts, J. L. The influence of bacterial diet on fat storage in C.
570 elegans. *PLoS One* **4**, e7545, doi:10.1371/journal.pone.0007545 (2009).
571 33 Perez, C. L. & Van Gilst, M. R. A 13C isotope labeling strategy reveals the influence of
572 insulin signaling on lipogenesis in C. elegans. *Cell Metab* **8**, 266-274, doi:S1550-
573 4131(08)00248-9 [pii] 10.1016/j.cmet.2008.08.007 (2008).
574 34 Kirkwood, T. B. & Holliday, R. The evolution of ageing and longevity. *Proc R Soc Lond B*
575 *Biol Sci* **205**, 531-546 (1979).
576 35 Narbonne, P. & Roy, R. Caenorhabditis elegans dauers need LKB1/AMPK to ration lipid
577 reserves and ensure long-term survival. *Nature* **457**, 210-214, doi:nature07536 [pii]
578 10.1038/nature07536 (2009).
579 36 Miller, H. *et al.* Genetic interaction with temperature is an important determinant of
580 nematode longevity. *Aging Cell* **16**, 1425-1429, doi:10.1111/acel.12658 (2017).
581 37 Lapierre, L. R., Kumsta, C., Sandri, M., Ballabio, A. & Hansen, M. Transcriptional and
582 epigenetic regulation of autophagy in aging. *Autophagy* **11**, 867-880,
583 doi:10.1080/15548627.2015.1034410 (2015).
584 38 Dupuy, D. *et al.* Genome-scale analysis of in vivo spatiotemporal promoter activity in
585 Caenorhabditis elegans. *Nat Biotechnol* **25**, 663-668, doi:10.1038/nbt1305 (2007).

586 39 Kelmer Sacramento, E. *et al.* Reduced proteasome activity in the aging brain results in
587 ribosome stoichiometry loss and aggregation. *Mol Syst Biol* **16**, e9596,
588 doi:10.15252/msb.20209596 (2020).
589 40 Guo, B. *et al.* Genome-wide screen identifies signaling pathways that regulate autophagy
590 during Caenorhabditis elegans development. *EMBO Rep* **15**, 705-713,
591 doi:10.1002/embr.201338310 (2014).
592 41 Robichaud, S. *et al.* Identification of novel lipid droplet factors that regulate lipophagy and
593 cholesterol efflux in macrophage foam cells. *Autophagy* **17**, 3671-3689,
594 doi:10.1080/15548627.2021.1886839 (2021).
595 42 Zhang, P. *et al.* Proteomic study and marker protein identification of Caenorhabditis
596 elegans lipid droplets. *Mol Cell Proteomics* **11**, 317-328, doi:10.1074/mcp.M111.016345
597 (2012).
598 43 Vrablik, T. L., Petyuk, V. A., Larson, E. M., Smith, R. D. & Watts, J. L. Lipidomic and
599 proteomic analysis of Caenorhabditis elegans lipid droplets and identification of ACS-4 as
600 a lipid droplet-associated protein. *Biochim Biophys Acta* **1851**, 1337-1345,
601 doi:10.1016/j.bbalip.2015.06.004 (2015).
602 44 Zechner, R., Kienesberger, P. C., Haemmerle, G., Zimmermann, R. & Lass, A. Adipose
603 triglyceride lipase and the lipolytic catabolism of cellular fat stores. *J Lipid Res* **50**, 3-21,
604 doi:10.1194/jlr.R800031-JLR200 (2009).
605 45 Lee, J. H. *et al.* Lipid droplet protein LID-1 mediates ATGL-1-dependent lipolysis during
606 fasting in Caenorhabditis elegans. *Mol Cell Biol* **34**, 4165-4176, doi:10.1128/MCB.00722-
607 14 (2014).
608 46 Olzmann, J. A. & Carvalho, P. Dynamics and functions of lipid droplets. *Nat Rev Mol Cell*
609 *Biol* **20**, 137-155, doi:10.1038/s41580-018-0085-z (2019).

610 47 Denzel, M. S., Lapierre, L. R. & Mack, H. I. D. Emerging topics in C. elegans aging
611 research: Transcriptional regulation, stress response and epigenetics. *Mech Ageing Dev*
612 **177**, 4-21, doi:10.1016/j.mad.2018.08.001 (2019).
613 48 Moldavski, O. *et al.* Lipid Droplets Are Essential for Efficient Clearance of Cytosolic
614 Inclusion Bodies. *Dev Cell* **33**, 603-610, doi:10.1016/j.devcel.2015.04.015 (2015).
615 49 Mejhert, N. *et al.* Partitioning of MLX-Family Transcription Factors to Lipid Droplets
616 Regulates Metabolic Gene Expression. *Mol Cell* **77**, 1251-1264 e1259,
617 doi:10.1016/j.molcel.2020.01.014 (2020).
618 50 Zhang, S. O. *et al.* Genetic and dietary regulation of lipid droplet expansion in
619 Caenorhabditis elegans. *Proc Natl Acad Sci U S A* **107**, 4640-4645,
620 doi:10.1073/pnas.0912308107 (2010).
621 51 Zaarur, N. *et al.* ATGL-1 mediates the effect of dietary restriction and the insulin/IGF-1
622 signaling pathway on longevity in C. elegans. *Mol Metab* **27**, 75-82,
623 doi:10.1016/j.molmet.2019.07.001 (2019).
624 52 Olzmann, J. A., Richter, C. M. & Kopito, R. R. Spatial regulation of UBXD8 and p97/VCP
625 controls ATGL-mediated lipid droplet turnover. *Proc Natl Acad Sci U S A* **110**, 1345-1350,
626 doi:10.1073/pnas.1213738110 (2013).
627 53 Wu, X. & Rapoport, T. A. Mechanistic insights into ER-associated protein degradation.
628 *Curr Opin Cell Biol* **53**, 22-28, doi:10.1016/j.ceb.2018.04.004 (2018).
629 54 Bug, M. & Meyer, H. Expanding into new markets--VCP/p97 in endocytosis and
630 autophagy. *J Struct Biol* **179**, 78-82, doi:10.1016/j.jsb.2012.03.003 (2012).
631 55 Hill, S. M. *et al.* VCP/p97 regulates Beclin-1-dependent autophagy initiation. *Nat Chem*
632 *Biol* **17**, 448-455, doi:10.1038/s41589-020-00726-x (2021).
633 56 Vembar, S. S. & Brodsky, J. L. One step at a time: endoplasmic reticulum-associated
634 degradation. *Nat Rev Mol Cell Biol* **9**, 944-957, doi:10.1038/nrm2546 (2008).

635 57 Demishtein, A. *et al.* SQSTM1/p62-mediated autophagy compensates for loss of
636 proteasome polyubiquitin recruiting capacity. *Autophagy* **13**, 1697-1708,
637 doi:10.1080/15548627.2017.1356549 (2017).
638 58 Korolchuk, V. I., Mansilla, A., Menzies, F. M. & Rubinsztein, D. C. Autophagy inhibition
639 compromises degradation of ubiquitin-proteasome pathway substrates. *Mol Cell* **33**, 517-
640 527, doi:10.1016/j.molcel.2009.01.021 (2009).
641 59 Mohri-Shiomi, A. & Garsin, D. A. Insulin signaling and the heat shock response modulate
642 protein homeostasis in the Caenorhabditis elegans intestine during infection. *J Biol Chem*
643 **283**, 194-201, doi:10.1074/jbc.M707956200 (2008).
644 60 McColl, G. *et al.* Utility of an improved model of amyloid-beta (Abeta(1)(-)(4)(2)) toxicity in
645 Caenorhabditis elegans for drug screening for Alzheimer's disease. *Mol Neurodegener* **7**,
646 57, doi:10.1186/1750-1326-7-57 (2012).
647 61 Franz, A., Ackermann, L. & Hoppe, T. Create and preserve: proteostasis in development
648 and aging is governed by Cdc48/p97/VCP. *Biochim Biophys Acta* **1843**, 205-215,
649 doi:10.1016/j.bbamcr.2013.03.031 (2014).
650 62 Roberts, M. A. & Olzmann, J. A. Protein Quality Control and Lipid Droplet Metabolism.
651 *Annu Rev Cell Dev Biol* **36**, 115-139, doi:10.1146/annurev-cellbio-031320-101827 (2020).
652 63 Bersuker, K. & Olzmann, J. A. Establishing the lipid droplet proteome: Mechanisms of lipid
653 droplet protein targeting and degradation. *Biochim Biophys Acta Mol Cell Biol Lipids* **1862**,
654 1166-1177, doi:10.1016/j.bbalip.2017.06.006 (2017).
655 64 Galluzzi, L., Bravo-San Pedro, J. M., Levine, B., Green, D. R. & Kroemer, G.
656 Pharmacological modulation of autophagy: therapeutic potential and persisting obstacles.
657 *Nat Rev Drug Discov* **16**, 487-511, doi:10.1038/nrd.2017.22 (2017).
658 65 Zaffagnini, G. *et al.* Phasing out the bad-How SQSTM1/p62 sequesters ubiquitinated
659 proteins for degradation by autophagy. *Autophagy* **14**, 1280-1282,
660 doi:10.1080/15548627.2018.1462079 (2018).

661 66 Baskoylu, S. N. *et al.* Disrupted autophagy and neuronal dysfunction in C. elegans knockin
662 models of FUS amyotrophic lateral sclerosis. *Cell Rep* **38**, 110195,
663 doi:10.1016/j.celrep.2021.110195 (2022).
664 67 Zaffagnini, G. *et al.* p62 filaments capture and present ubiquitinated cargos for autophagy.
665 *EMBO J* **37**, doi:10.15252/embj.201798308 (2018).
666 68 Hansen, M., Flatt, T. & Aguilaniu, H. Reproduction, fat metabolism, and life span: what is
667 the connection? *Cell Metab* **17**, 10-19, doi:10.1016/j.cmet.2012.12.003 (2013).
668 69 Silvestrini, M. J. *et al.* Nuclear Export Inhibition Enhances HLH-30/TFEB Activity,
669 Autophagy, and Lifespan. *Cell Rep* **23**, 1915-1921, doi:10.1016/j.celrep.2018.04.063
670 (2018).
671 70 Littlejohn, N. K., Seban, N., Liu, C. C. & Srinivasan, S. A feedback loop governs the
672 relationship between lipid metabolism and longevity. *eLife* **9**, doi:10.7554/eLife.58815
673 (2020).
674 71 Ding, L. *et al.* Peroxisomal beta-oxidation acts as a sensor for intracellular fatty acids and
675 regulates lipolysis. *Nat Metab* **3**, 1648-1661, doi:10.1038/s42255-021-00489-2 (2021).
676 72 Schmitz, G. & Grandl, M. Lipid homeostasis in macrophages - implications for
677 atherosclerosis. *Rev Physiol Biochem Pharmacol* **160**, 93-125,
678 doi:10.1007/112_2008_802 (2008).
679 73 Marschallinger, J. *et al.* Lipid-droplet-accumulating microglia represent a dysfunctional
680 and proinflammatory state in the aging brain. *Nat Neurosci* **23**, 194-208,
681 doi:10.1038/s41593-019-0566-1 (2020).
682 74 Nguyen, T. B. *et al.* DGAT1-Dependent Lipid Droplet Biogenesis Protects Mitochondrial
683 Function during Starvation-Induced Autophagy. *Dev Cell* **42**, 9-21 e25,
684 doi:10.1016/j.devcel.2017.06.003 (2017).
685 75 Di Paolo, G. & Kim, T. W. Linking lipids to Alzheimer's disease: cholesterol and beyond.
686 *Nat Rev Neurosci* **12**, 284-296, doi:10.1038/nrn3012 (2011).

687 76 Inloes, J. M. *et al.* The hereditary spastic paraplegia-related enzyme DDHD2 is a principal
688 brain triglyceride lipase. *Proc Natl Acad Sci U S A* **111**, 14924-14929,
689 doi:10.1073/pnas.1413706111 (2014).
690 77 Yang, L. *et al.* Neuronal lipolysis participates in PUFA-mediated neural function and
691 neurodegeneration. *EMBO Rep* **21**, e50214, doi:10.15252/embr.202050214 (2020).
692 78 Nuriel, T. *et al.* Neuronal hyperactivity due to loss of inhibitory tone in APOE4 mice lacking
693 Alzheimer's disease-like pathology. *Nat Commun* **8**, 1464, doi:10.1038/s41467-017-
694 01444-0 (2017).
695 79 Labbadia, J. & Morimoto, R. I. The biology of proteostasis in aging and disease. *Annu Rev*
696 *Biochem* **84**, 435-464, doi:10.1146/annurev-biochem-060614-033955 (2015).
697 80 Brenner, S. The genetics of Caenorhabditis elegans. *Genetics* **77**, 71-94 (1974).
698 81 Stiernagle, T. Maintenance of C. elegans. *WormBook*, 1-11,
699 doi:10.1895/wormbook.1.101.1 (2006).
700 82 Kamath, R. S. *et al.* Systematic functional analysis of the Caenorhabditis elegans genome
701 using RNAi. *Nature* **421**, 231-237 (2003).
702 83 Hansen, M., Hsu, A. L., Dillin, A. & Kenyon, C. New genes tied to endocrine, metabolic,
703 and dietary regulation of lifespan from a Caenorhabditis elegans genomic RNAi screen.
704 *PLoS Genet* **1**, 119-128 (2005).
705 84 Holdorf, A. D. *et al.* WormCat: An Online Tool for Annotation and Visualization of
706 Caenorhabditis elegans Genome-Scale Data. *Genetics* **214**, 279-294,
707 doi:10.1534/genetics.119.302919 (2020).
708

Figure 1

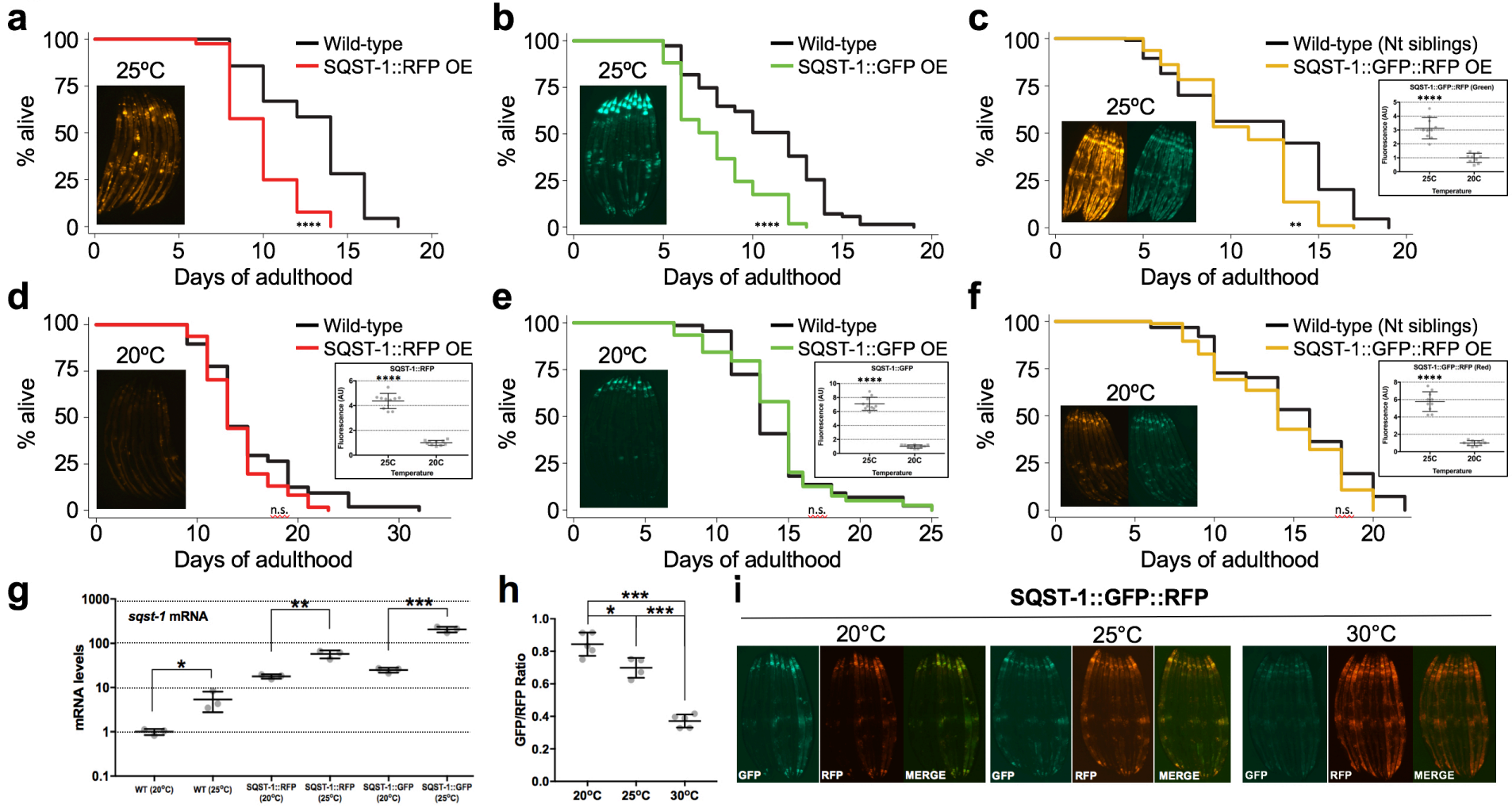
a
25ºC
Wild-type
SQST-1::RFP OE
% alive
Days of adulthood
****
b
25ºC
Wild-type
SQST-1::GFP OE
****
c
25ºC
Wild-type (Nt siblings)
SQST-1::GFP::RFP OE
SQST-1::GFP::RFP (Green)
Fluorescence (AU)
Temperature
**
d
20ºC
Wild-type
SQST-1::RFP OE
SQST-1::RFP
n.s.
e
20ºC
Wild-type
SQST-1::GFP OE
SQST-1::GFP
f
20ºC
Wild-type (Nt siblings)
SQST-1::GFP::RFP OE
SQST-1::GFP::RFP (Red)
g
sqst-1 mRNA
mRNA levels
WT (20ºC)
WT (25ºC)
SQST-1::RFP (20ºC)
SQST-1::RFP (25ºC)
SQST-1::GFP (20ºC)
SQST-1::GFP (25ºC)
h
GFP/RFP Ratio
20ºC
25ºC
30ºC
i
SQST-1::GFP::RFP
20°C
25°C
30°C
GFP
RFP
MERGE

Figure 1. SQST-1 dynamics and lifespan modulation is temperature-dependent in *C. elegans*
a-f. Lifespan analysis of wild-type animals and animals over-expressing SQST-1 fused to RFP, GFP or GFP::RFP fed OP50 *E. coli*, developmentally raised at 20°C and then grown at 25°C (**a-c**) or 20°C (**d-f**) during adulthood (n=100). Insets include corresponding representative images of transgenic animals at Day 5 of adulthood, and quantified fluorescence, ±SD *t-test ****p<0.001*. Nt: Non transgenic. **g.** *sqst-1* mRNA levels in wild-type and transgenic animals were quantified by qPCR. Biological triplicates ±SD *t-test *p<0.05, **p<0.01, ***p<0.001* **h.** Levels of GFP and RFP were measured in transgenic tandem SQST-1::GFP::RFP animals (leveraging the pH sensitivity of GFP to visualize SQST-1 accumulation in autolysosome) after incubating Day 1 animals at 20°C, 25°C or 30°C for 24 hours. Average of 10 worms per image. n=5 images per condition ±SD *ANOVA *p<0.05, **p<0.01, ***p<0.001.* Difference in signal between GFP and RFP is due to the low pH sensitivity of GFP. Thus, RFP-only signal represents SQST-1 protein in autolysosomes. **i.** Representative images of transgenic animals (quantified in h.) incubated at 20°C, 25°C or 30°C for 24 hours. Details about lifespan analyses and repeats are available in Supplemental Table 4, Mantel-Cox log-rank. n.s.: not significant, ***p<0.01,****p<0.001*.

Figure 2

a

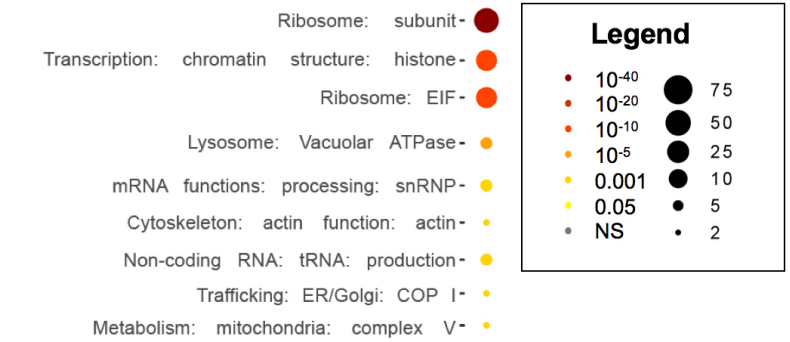

b

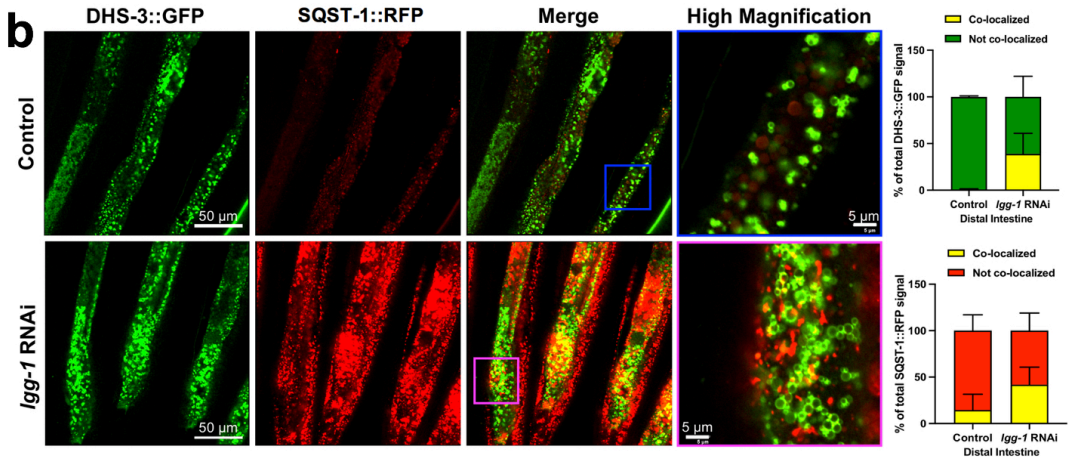

c

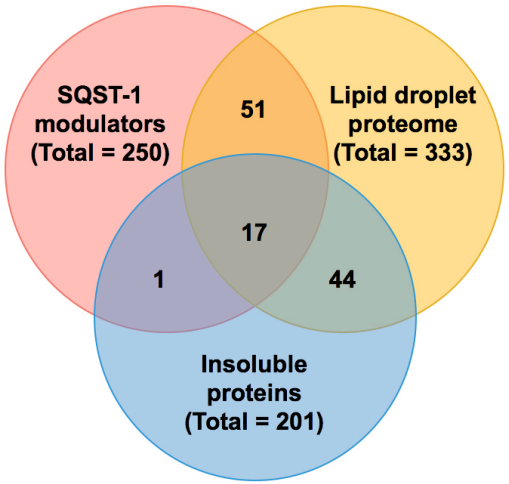

SQST-1 modulators that aggregate with age and bind lipid droplets	
inf-1	*rps-11*
rpl-17	*rps-14*
rpl-19	***rps-16***
rpl-23	*rps-23*
rpl-31	*rps-28*
rpl-7	*rps-3*
rpl-9	*rps-5*
rps-0	***hsp-1***
	pab-1

d

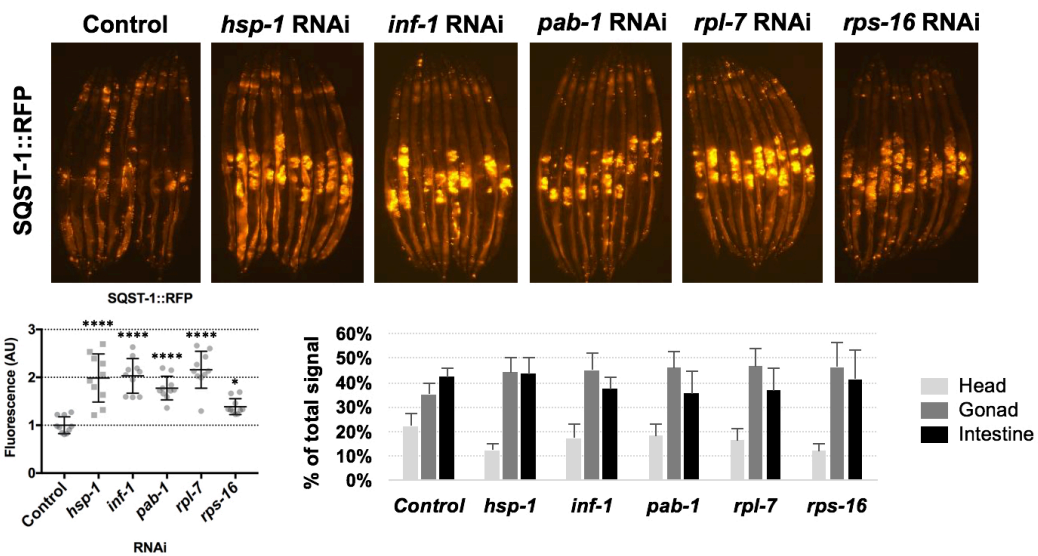

Figure 2. SQST-1 regulators include proteins that bind lipid droplets and that aggregate with age
a. Pathway enrichment of genes that regulate SQST-1 levels using WormCat[77]. **b.** SQST-1::RFP accumulates after autophagy is inhibited by *lgg-1* silencing for 3 days during adulthood. Representative confocal microscopy image of the distal intestine of animals expressing both SQST-1::RFP and the lipid droplet-resident protein DHS-3 fused to GFP, subjected to *lgg-1* silencing for 3 days during adulthood. The co-localization between DHS-3::GFP and SQST-1::GFP is quantified. **c.** Overlap of SQST-1 regulators with age-dependent aggregating proteins[2] and lipid droplet-associated proteins[40]. **d.** Representative images of gene silencing of a set of overlapping SQST-1 regulators during adulthood for 3 days in animals over-expressing SQST-1::RFP. Fluorescence and tissue distribution quantified ±SD *ANOVA* $*p<0.05$, $****p<0.001$. Details about SQST-1 regulators are available in Supplemental Tables 1 and 2.

Figure 3

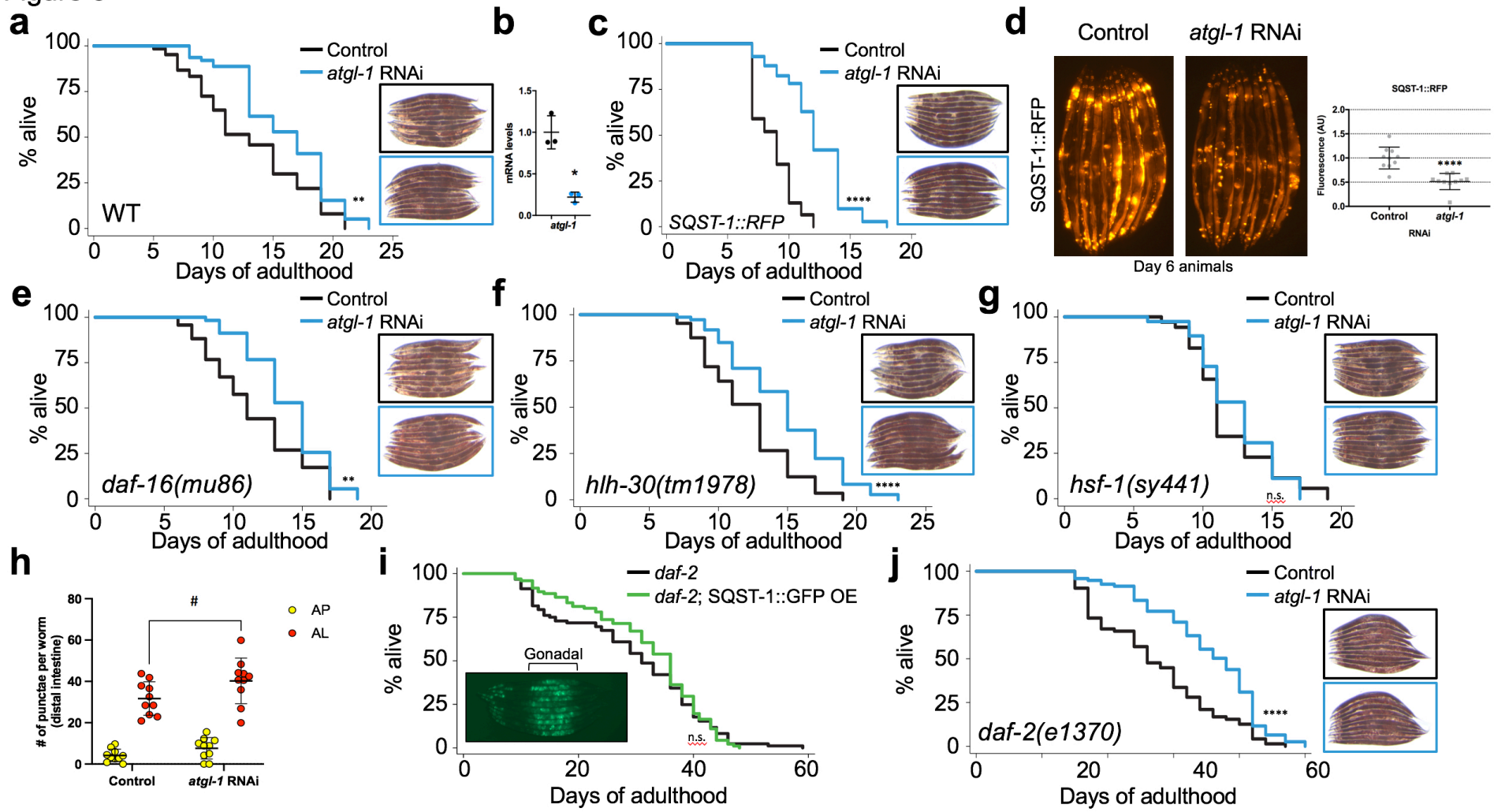
a
% alive
Days of adulthood
Control
atgl-1 RNAi
WT
**
b
mRNA levels
atgl-1
*
c
SQST-1::RFP
****
d
Control
atgl-1 RNAi
SQST-1::RFP
Day 6 animals
Fluorescence (AU)
e
daf-16(mu86)
f
hlh-30(tm1978)
g
hsf-1(sy441)
n.s.
h
# of punctae per worm (distal intestine)
AP
AL
#
i
daf-2
daf-2; SQST-1::GFP OE
Gonadal
j
daf-2(e1370)

Figure 3. Silencing *atgl-1* extends lifespan and reduces SQST-1 accumulation in *C. elegans*
a. Lifespan analysis of wild-type animals and **c.** animals over-expressing SQST-1::RFP raised at 20°C on OP50 *E. coli* and then grown at 25°C during adulthood on control bacteria or bacteria expressing dsRNA against *atgl-1* (n=100). Corresponding images of Day 5 animals stained with Oil-Red-O demonstrating intestinal lipid store accretion under *atgl-1* RNAi (blue borders). **b.** Levels of *atgl-1* mRNA measured by qPCR showing efficient silencing after 3 days on *atgl-1* RNAi (Black: Control RNAi, Blue: *atgl-1* RNAi*)*. Biological triplicates *t*-test $^{*}p<0.05$ **d.** Representative fluorescence images taken after Day 1 animals over-expressing SQST-1::RFP and DHS-3::GFP were fed control bacteria or bacteria expressing dsRNA against *atgl-1* for 5 days at 25°C. **e-g.** Lifespan analysis of *daf-16(mu86)*, *hlh-30(tm1978),* and *hsf-1(sy441)* mutants raised at 20°C on OP50 *E. coli* and then grown at 25°C during adulthood on control bacteria or bacteria expressing dsRNA against *atgl-1* (n=100). Corresponding images of Day 5 animals stained with ORO demonstrating intestinal lipid store accretion under *atgl-1* RNAi (blue borders). **h.** Levels of autophagosomes and autolysosomes were measured in animals expressing the tandem reporter mCherry::GFP::LGG-1[7] after feeding Day 1 animals with control bacteria or bacteria expressing dsRNA against *atgl-1* for 2 days at 25°C. n=10 per condition ±SD *t*-test $^{\#}p<0.06$ **i.** Lifespan analysis of *daf-2(e1370)* and *daf-2;SQST-1::GFP* animals raised at 20°C and then grown at 25°C during adulthood on OP50 *E. coli* (with representative image of Day 5 animals, comparative image of wild-type animals in Figure 1b). **j.** *daf-2(e1370)* animals were raised at 20°C on OP50 *E. coli* and then grown at 25°C during adulthood on control bacteria or bacteria expressing dsRNA against *atgl-1* (n=100). Corresponding images of Day 5 animals stained with ORO demonstrating intestinal lipid store accretion under *atgl-1* RNAi (blue borders). Details about lifespan analyses and repeats are available in Supplemental Tables 3 and 4, Mantel-Cox log-rank. n.s.: not significant, $^{**}p<0.01$, $^{****}p<0.001$..

Figure 4

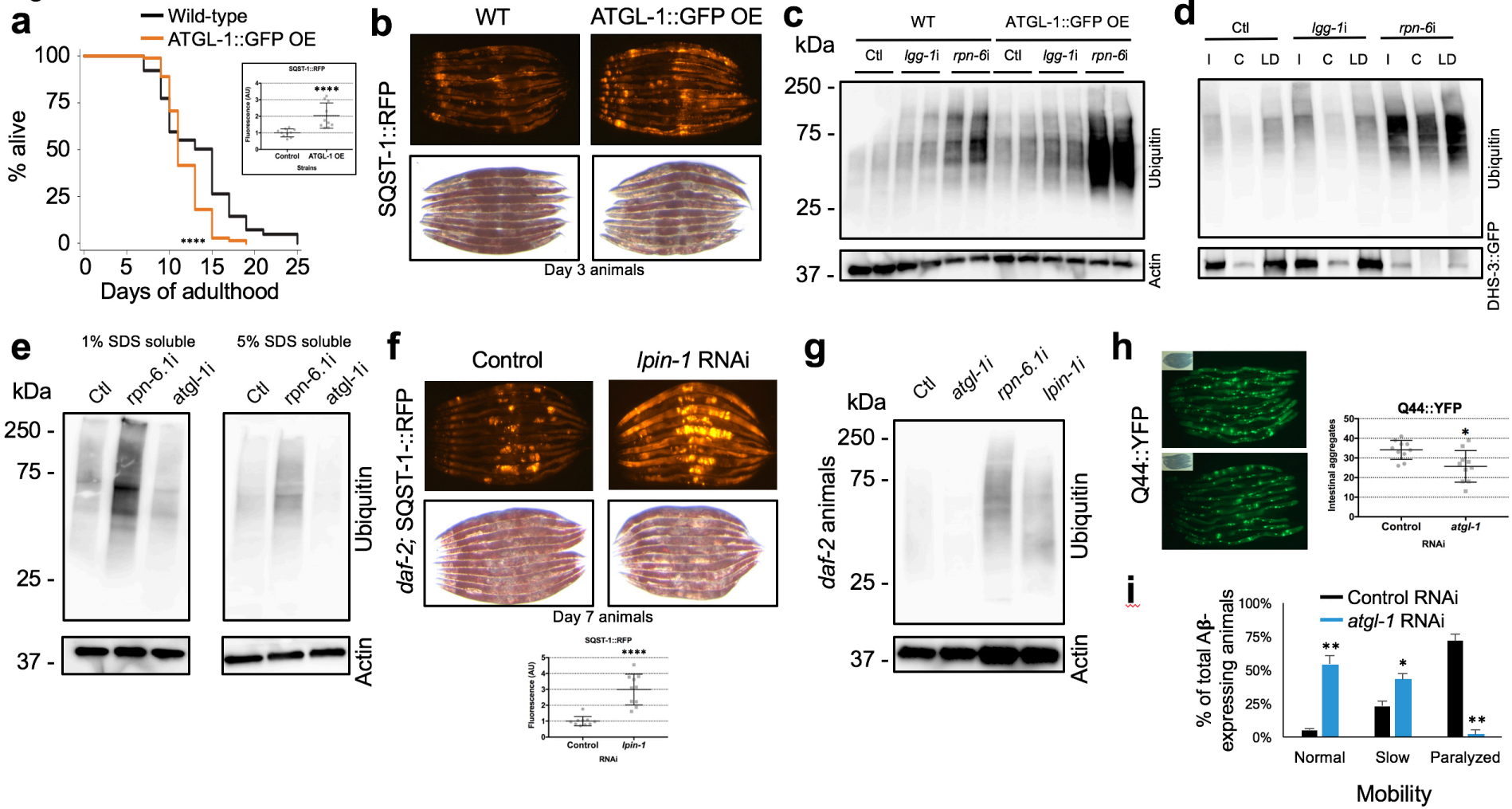
a
Wild-type
ATGL-1::GFP OE
% alive
Days of adulthood
SQST-1::RFP
Control
ATGL-1 OE
Strains
b
WT
ATGL-1::GFP OE
SQST-1::RFP
Day 3 animals
c
WT
ATGL-1::GFP OE
kDa
Ctl
lgg-1i
rpn-6i
Ubiquitin
Actin
d
Ctl
lgg-1i
rpn-6i
I
C
LD
Ubiquitin
DHS-3::GFP
e
1% SDS soluble
5% SDS soluble
kDa
Ctl
rpn-6.1i
atgl-1i
Ubiquitin
Actin
f
Control
lpin-1 RNAi
daf-2; SQST-1::RFP
Day 7 animals
SQST-1::RFP
Control
lpin-1
RNAi
g
kDa
Ctl
atgl-1i
rpn-6.1i
lpin-1i
daf-2 animals
Ubiquitin
Actin
h
Q44::YFP
Intestinal aggregates
Control
atgl-1
RNAi
i
Control RNAi
atgl-1 RNAi
% of total Aβ-expressing animals
Normal
Slow
Paralyzed
Mobility

Figure 4. Lipid droplets modulate protein ubiquitination levels and enhance proteostasis
a. Lifespan analysis of wild-type and transgenic animals over-expressing ATGL-1::GFP developmentally raised at 20°C and then grown at 25°C during adulthood on OP50 *E. coli* (n=100). **b.** Levels of RFP signal and lipid droplets from Day 3 animals over-expressing SQST-1::RFP in wild-type or transgenic ATGL-1::GFP over-expressing background. **c.** Wild-type and ATGL-1::GFP over-expressing animals were raised at 20°C and then grown at 25°C during adulthood on control bacteria (Ctl) or bacteria expressing dsRNA against autophagy gene *lgg-1* or proteasome subunit gene *rpn-6.1* for 2 days. Levels of ubiquitinated proteins and actin were visualized by immunAnimals expressing lipid droplet-resident protein DHS-3 fused to GFP were raised at 20°C and then grown at 25°C during adulthood on control bacteria or bacteria expressing RNAi against *lgg-1* or *rpn-6* for 4 days. Levels of ubiquitinated proteins and DHS-3::GFP were visualized by immunoblotting from total input (I), cytosol (C) and lipid droplet (LD) fractions (comparative % loaded between fractions, i.e. 10%). oblotting. Biological replicates shown. **d. e.** Day 1 wild-type animals were fed control bacteria or bacteria expressing dsRNA against *rpn-6* or *atgl-1* for 3 days and ubiquitination levels were detected by immunoblotting. **f.** Levels of RFP signal and lipid droplets in Day 7 *daf-2* animals over-expressing SQST-1::RFP and fed control bacteria or bacteria expressing dsRNA against *lpin-1* during adulthood. **g.** Day 1 *daf-2* animals were fed control bacteria or bacteria expressing dsRNA against *atgl-1, rpn-6* or *lpin-1* for 5 days at 25°C and ubiquitination levels were detected by immunoblotting. **h.** Nematodes expressing intestinally Q44::YFP were grown at at 20°C on OP50 *E. coli* and fed control bacteria or bacteria expressing dsRNA against *atgl-1* at Day 1 of adulthood for 4 days at 25°C, followed by quantification of intestinal aggregates. ±SD *t*-test *$*p<0.05$.* **i.** Nematodes expressing heat-inducible human A**β**-42 were grown at 20°C on OP50 *E. coli* and fed control bacteria or bacteria expressing dsRNA against *atgl-1* at Day 1 of adulthood for 2 days at 25°C. Paralysis was scored thereafter. Triplicates of n=100 each, ±SD *t*-test *$*p<0.05$, $**p<0.01$.*

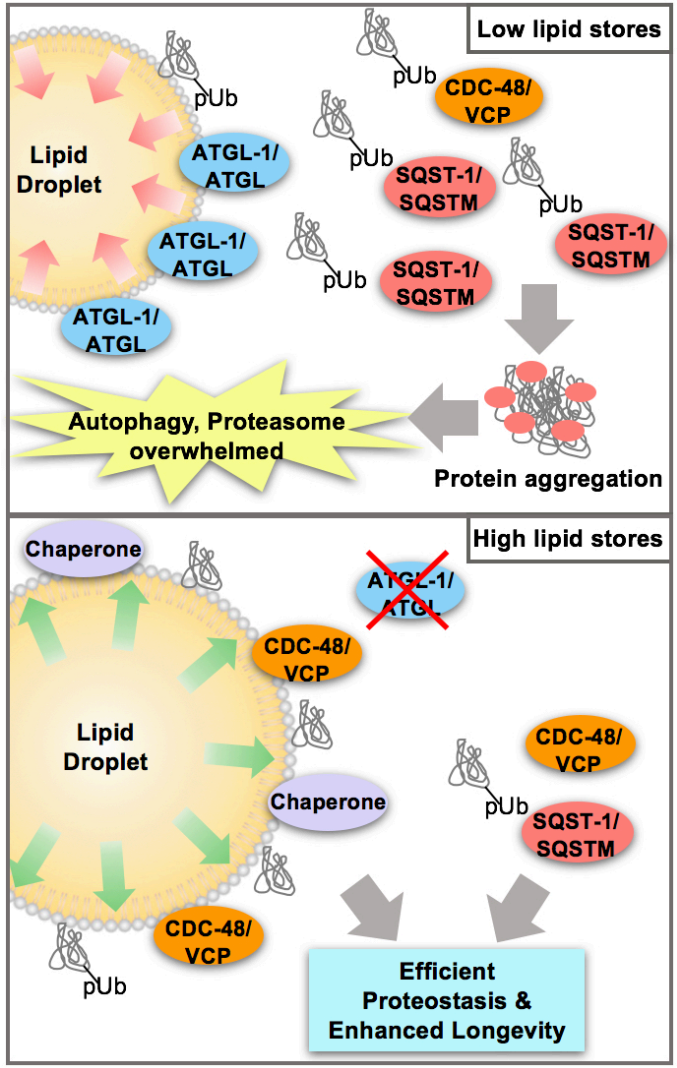
Low lipid stores
Lipid Droplet
ATGL-1/ ATGL
ATGL-1/ ATGL
ATGL-1/ ATGL
pUb
pUb
pUb
pUb
pUb
CDC-48/ VCP
SQST-1/ SQSTM
SQST-1/ SQSTM
SQST-1/ SQSTM
Autophagy, Proteasome overwhelmed
Protein aggregation
High lipid stores
Chaperone
ATGL-1/ ATGL
CDC-48/ VCP
Lipid Droplet
Chaperone
CDC-48/ VCP
pUb
SQST-1/ SQSTM
CDC-48/ VCP
pUb
Efficient Proteostasis & Enhanced Longevity

Figure 5. Lipid droplets buffer proteostasis by harboring proteins that challenge protein degradation pathways. When lipid stores are low, ubiquitinated proteins accumulate and eventually overwhelm the proteasomal system and selective autophagy receptors such as SQST-1. High lipid droplet content increases the capacity of cells to stabilize proteins (in conjunction with CDC-48 and HSF-1-regulated chaperones, such as HSP-1) that would otherwise accumulate and aggregate. As proteostasis declines with age, lipid droplets can facilitate autophagic degradation and stabilize the proteome, which prevents the burdening of selective autophagy.